Size And Chirality Effects On Raman Spectrum Of Double-Wall Carbon Nanotube Bundle

K. Sbai[(1)], A. Rahmani[(1)], H. Chadli[(1)] and J. L. Sauvajol[(2)]

(1) Equipe de Physique Informatique et Modélisation des Systèmes, Université MY Ismaïl, Faculté des Science, BP 11201, 50000 Meknès, Morocco.

(2) Laboratoire des Colloides, Verres et Nanomatériaux (UMR CNRS 5587) , CP026, Université Montpellier II, 34095 Montpellier Cedex 5, France.
Corresponding Author : email abdelali@fs-umi.ac.ma.

We study the tube size and bundling effects on Raman active breathing-like phonon modes (BLM) and tangential-like phonon mode (TLM) of double-walled carbon nanotubes (DWCNT) in the framework of the bond polarization theory, and use the spectral moment's method. The Raman active modes are calculated for different diameter and chirality of the inner and outer DWCNT tubes. The dependence of the Raman spectrum of bundles of identical DWCNTs as a function of the size of the bundle is analysed and additional breathing-like modes are predicted in DWCNT bundle of finite size.

Keywords: carbon Nanotube, Raman spectroscopy, spectral moment method, simulation.

I. INTRODUCTION

Recently, double-wall carbon nanotubes (DWCNT), which consist of two concentric cylindrical graphene layers, have been successfully synthesized by catalytic chemical vapour deposition [1, 2, 3] and by the thermal conversion of C_{60} encapsulated in single-wall carbon nanotubes (SWCNT) [4]. Double-wall carbon nanotubes are the subject of intense studies knowing their promising applications.

Raman scattering is a useful technique to study the one-dimensional properties of carbon nanotubes, since it can probe both the phonon spectrum and the electronic structure [5]. In past years, Raman scattering investigations mostly focused on SWCNTs.

In previous work [6], we used the spectral moment method in the framework of the bond-polarization theory to calculate non-resonant polarized Raman spectrum of both chiral and achiral SWCNTs as a function of their diameter and length. Raman experiments on DWCNTs have also been performed. The data were mostly analysed on the basis of the theoretical predictions stated in the case of SWCNTs. A detailed Raman investigation of DWCNTs prepared from thermal conversion of C_{60} encapsulated in SWCNTs has been reported [4,17]. The Raman spectra measured on samples and prepared by the catalytic chemical vapor deposition method (CCVD) have been also reported [7]. The authors use the linear relation between the frequency of the totally symmetric radial breathing mode (the so-called RBM) and the inverse of the diameter, found in SWCNT's, $\omega_{RBM} = A/D$, to assign the different couples of inner and outer tubes occurred in their samples. The diameter D of the previous expression is D_{inner} for the inner tube and D_{outer} for the outer tube with $D_{outer}=D_{inner}+2d$, where d is the distance between the inner and outer tubes. In SWCNT, the prefactor A is known to be model dependent: A=22.3 cm^{-1}Å [8], 23.4 cm^{-1}Å [9], 23.6 cm^{-1}Å [10]. The difference between experimental and predicted RBLM frequencies is understood in terms of the reduced interlayer distance between the inner and the outer tubes due to the tube-tube interaction. In their assignment, neglecting the tube-tube interaction, the authors take the average value A=23.4 cm^{-1}Å.

DWCNT prepared by floating catalyst CVD method were studied by Raman scattering by Ci *et al.* [11]. The assignment of the inner tube and outer tube is done according to the equation $\omega_{RBM} = 23.8/D^{0.93}$. This latter expression takes into account the tube-tube interaction [12].

In this paper we present calculations of the Raman active modes of isolated DWCNT of infinite and finite lengths, and of DWCNT

bundles of different sizes in the breathing-like modes (BLM) and tangential-like modes (TLM) ranges. These calculations have been performed in the framework of the bond-polarization theory using the spectral moments method [6, 13].

II. MODELS AND METHOD

A double-wall carbon nanotube is a special case of multiwall tubes consisting of only two concentrics SWCNT's. The DWCNT walls are assumed to be at a distance d close to 3.4 Å and whose diameters are D_{in}=D and D_{out}=D+d. We recall that the diameter of a carbon nanotube of chirality (n, m) is given by $D=a[3(m^2+mn+n^2)]^{1/2}/\pi$, where a=1.42 Å. Let us note that DWCNT is made up of an internal tube (n, m) and an external tube (k, l) as (n, m)@(k,l).

As for SWCNT's, the DWCNT's can be packed to form a bundle. For finite-size bundle, we assume that the DWCNT's were placed parallel one to each other on a finite-size hexagonal array of cell parameter $a_0=D_{out}+d_{t-t}$ to form concentric shells, with an intertube spacing d_{t-t} fixed to 3.2Å as for bundle of SWCNT's. The number of double-tubes per bundle is called N_t.

In this work, we calculate the Raman spectrum for single and bundle of DWCNT's with finite and infinite sizes. We consider that intratube interaction is represented by the force constants set used in our previous paper concerning the Raman spectrum in isolated single-wall carbon nanotubes [6]. A Lennard-Jones potential:

$$U_{LJ}=4\,\varepsilon[(\sigma/R)^{12}-(\sigma/R)^{6}]$$

is used to describe the intertube interactions for both SWCNT-SWCNT and DWCNT-DWCNT. We used the van der Waals parameters $\varepsilon = 2.964$ meV and $\sigma = 3.407$Å in all our calculations. To describe the coupling between vibrational modes and photons, we use the non-resonant bond-polarizability model. As in our previous works [6, 14, 18], the Raman intensities are calculated, using the spectral moments method [13], directly from the dynamical matrix without any diagonalization. The mode frequency is directly obtained from the position of the peak in the calculated Raman spectrum, the intensities are normalized and the Lorentzian linewidth is fixed at 1.7 cm^{-1}. We notice also that the Z (X) nanotube axis is along the z (x) axis of the laboratory reference frame and the laser beam is kept along the y axis. We consider that both incident and scattered polarizations are along the z axis and averaging over all tube orientations in space. More than 50000 atoms in carbon nanotubes are treated.

III. NUMERICAL RESULTS

In this section, we report the calculated Raman spectrum for infinite and finite isolated DWCNT, and for DWCNT bundles of different sizes. The dependence of the Raman spectrum as a function of tube diameter for the chiral@chiral DWCNTs is investigated.

For different DWCNTs the Lennard-Jones intertube interaction energy was minimized with respect to the interlayer separation, the relative angle of rotation of the layers around the tube axis and their relative translation along the tube axis. The optimal intertube gap is found around 3.4 Å. Calculations of the Raman spectrum, before and after energy minimization; do not show significative difference in the mode frequencies. This result was in agreement with that of Popov [15, 16] who found no significant differences between the BLM and TLM frequencies of the optimized and non-optimized DWCNTs in terms of relative angles of rotation and relative translation of the inner and outer tubes.

a) Infinite single DWCNT's

The calculations are performed on infinite DWCNT's of different diameters. To obtain infinite DWCNTs we applied periodic boundary conditions on unit cells of the considered nanotubes forming the system. To study the chirality of internal and externel tubes effects on the DWCNT Raman active-modes, we have considered different DWCNT walls combinations. Since DWCNT walls are assumed to be at a distance d=6.8 Å, the (n,n)@(n+5,n+5), (n,0)@(n+9,0) and (n,m)@(n+6,m+4) are the possible armchair, zigzag and chiral DWCNT's, respectively. In general, for chiral DWCNT's, we assume that all combinations with respect to intertube distance around this value are the possible systems. We observe that for all combinations, the RBLM region exhibits the same behaviour with two modes associated to internal and external tubes, whereas, the TLM region as expected is very sensitive to the DWCNT chirality.

In this study, we focus our interest on the Raman spectrum of chiral@chiral DWCNTs. These DWCNTs are identified as (n,m)@(n+6,m+4). In order to illustrate our results, the calculated Raman spectrum of (7,4)@(13,8), (9,6)@(15,10), and (13,8)@(19,12)

DWCNTs are shown in the RBLM (figure 1, left) and TLM (Figure 1, right) regions, respectively.

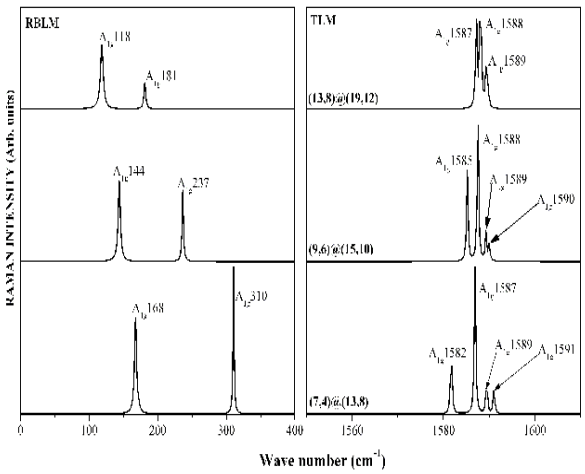

Figure 1: The calculated Raman spectrum of infinite (7,4)@(13,8), (9,6)@(15,10), and (13,8)@(19,12) DWCNTs in the RBLM (on the left) and TLM (on the right) regions.

In TLM region, all spectra display the peaks corresponding to A_{1g} modes for (n,m) and (k,l) tubes, respectively. For (9,6)@(15,10) DWCNT, for example, we found 1584, 1587, 1588 and 1589 cm^{-1} modes assigned to (9,6) and (15,10) tubes, respectively. In addition, when the tube diameter increases, we observe a shift for A_{1g} modes. As for TLM region, the RBLM one shows two modes associated to A_{1g} for each internal and external system tube. For example, in figure 1, the Raman spectrum of the (9,6)@(15,10) DWCNT displays peaks located at 236 cm^{-1} and 144 cm^{-1} (A_{1g}). As shown in figure 2, where we have

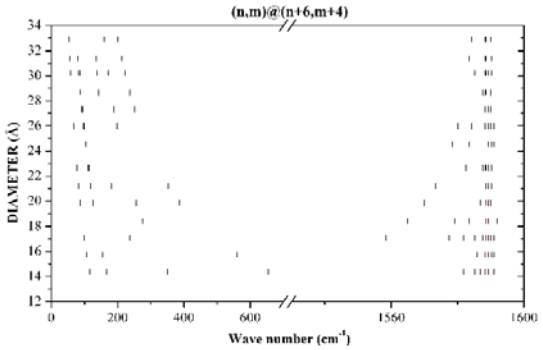

Figure 2: The frequency dependence of the Raman-active modes of an infinite (n,m)@(n+6,m+4) DWCNTs in terms of the tube diameter of the outer tube.

represented the outer tube diameter versus frequency, we observe a downshift for RBLM modes and a globally upshift of TLM modes with increasing diameter. Comparing with SWCNT Raman spectrum, we notice that the RBLM region of DWCNT's is characterized by an upshift of the frequency modes. The dependence with the diameter of RBLM modes in isolated infinite DWCNT can be obtained by the expression given in reference [18] stated for armchair@armchair DWCNT systems.

b) Finite single DWCNT's

To study effects of finite size on Raman spectrum of DWCNT's, we have performed calculations of ZZ spectrum of DWCNT's consisting of inner and outer tubes of different lengths. In figure 3, we report in the case of (9,6)@(15,10) DWCNT, with approximatively the same inner and outer length tubes, the RBLM and intermediate regions (on the left) and TLM region (on the right) of ZZ Raman spectrum for three lengths: L ≈ 74 Å, 149 Å and 297 Å.

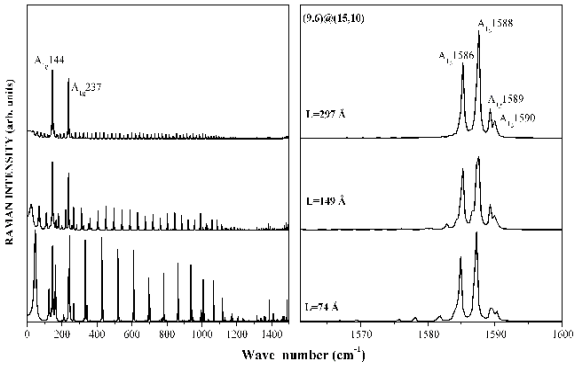

Figure 3: The ZZ calculated Raman spectrum of infinite (9,6)@(15,10) DWCNT of different lengths in RBLM and intermediate (on the left) and TLM (in the right) regions.

As for SWCNT's length dependence, we observe that besides observed modes (A_{1g}144, 236, 1584, 1587, 1588 and 1589 cm^{-1}) in infinite DWCNT's, a large number of additional peaks related to the finite size of the system occur in all regions. The intensity of these peaks rapidly decreases when the length of tube increases. For very larger length one can produce the infinite DWCNT Raman spectrum. To study the effect of the difference in length between inner and outer tubes, we have calculated the ZZ Raman spectrum of (9,6)@(15,10) DWCNT for $L_{in}=0.25L_{out}$, $L_{in}=0.5L_{out}$, $L_{in}=L_{out}$, $L_{in}=1.25L_{out}$ and $L_{in}=1.5L_{out}$

(figure 4). To eliminate size effects, we have applied periodic boundary conditions on the finite tubes.

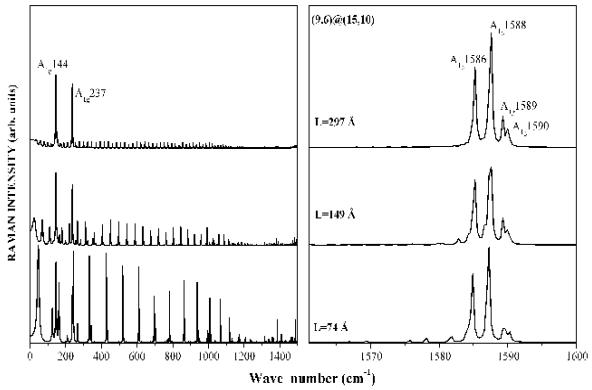

Figure 4: The ZZ calculated Raman spectrum of (9,6)@(15,10) DWCNT of five ratio $r=L_{in}/L_{out}$ between inner and outer tube lentghs: r =0.25, r=0.5, r=1, r=1.25 and r=1.5, in RBLM (on the left) and TLM (in the right) regions.

We observe that for $L_{in}<L_{out}$, the RBLM region is dominated by a double peaks around ω_s=132 cm^{-1} and ω_o=144 cm^{-1} which can be associated with the A^s_{1g} mode of SWCNT with an identical diameter to outer DWCNT tube and A^o_{1g} outer tube mode, respectively. When the length of the internal tube increases from L_{in} to L_{out} , the intensity of the double peaks shifts from the one located around ω_s to that located around ω_o. For $L_{in}=L_{out}$, an intensified single peak around ω_o remains. The intensity of the peak around ω_i=236 cm^{-1} assigned to A^i_{1g} inner DWCNT tube increases with L_{in} increasing. For $L_{in}>L_{out}$, we notice the appearance of three peaks around the frequency modes 219, 224-227 and 236 cm^{-1} with intensities depending on length difference between inner and outer tubes. The TLM regions are slightly affected by this length difference in peak positions relating to intensities.

c) Bundles of DWCNT's

To study effects of bundle finite size, we developed calculations of Raman intensity of bundles of different number of infinite DWCNT's. As mentioned above, in finite-size bundle, the DWCNT's were placed parallel to each other on a finite-size hexagonal array to form concentric shells.

Firstly, to show how Raman active modes of infinite bundle of DWCNT's evolve with diameter of the tube, we represent in figure 5 outer diameter versus frequency for chiral@chiral DWCNT's.

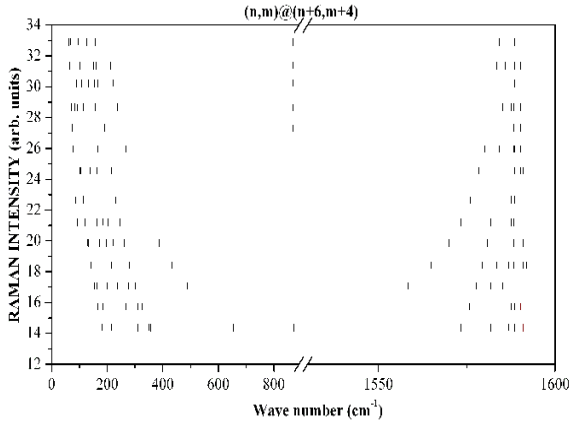

Figure 5: The frequency dependence of the Raman-active modes of an infinite bundle (n,m)@(n+6,m+4) DWCNTs in terms of the tube diameter of the outer tube.

We observe that the frequencies of the principal modes have a behaviour, generally according to the diameter of the tube, identical to that of single DWCNT's (figure 2). We notice that besides A^i_{1g} and A^o_{1g} modes there exist an additional breathing mode, noted here BM, in RBLM region. The intensity of this mode increases with increasing diameter. There is no significant difference between TLM regions of single and bundle of DWCNT's. Like single DWCNT's, an analysis of the RBLM frequency modes, variation with diameter, for DWCNT bundles, can be approximated by a two degrees polynomial [18].

Secondly, we are interested in bundling size effect on Raman spectrum. Calculations of ZZ polarized Raman spectrum for different bundles of DWCNT's of different chirality have been performed and qualitatively the same behaviour is observed. For example, in figure 6, we represent the RBLM regions of ZZ polarized Raman spectrum, for a typical (7,3)@(13,7) bundle of DWCNT's for five numbers of tubes N_t=1, 2, 7, 19 and 91 compared to DWCNT crystal one. Besides the A^o_{1g} frequency shifts from the frequency values 174 cm^{-1} for isolated DWCNT to 189 cm^{-1} for DWCNT crystal, additional peaks around this frequency mode, for given value of N_t, appeared: 127, 181 cm^{-1} for N_t=2, for example. When the size of the beam increases, additional peaks around A^o_{1g} are added with this last to form a single peak around 189 cm^{-1} for an infinite beam.

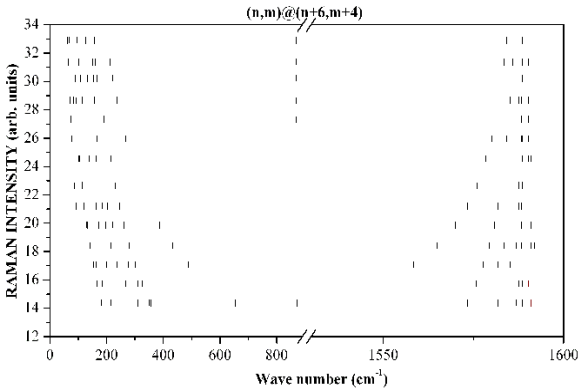

Figure_6: Dependence of the RBLM range of (7,3)@(13,7) DWCNT in terms of the number of tubes in the bundle. N_t= 1, 2, 7, 19, 61 and infinite.

We notice also between A^o_{1g} and A^i_{1g} the presence of other additional BM modes, for N_t >2: 248, 254 and 307 cm^{-1} for N_t =19, for example. These peaks disappear with increasing N_t and only the BM at frequency 255 cm^{-1} remain for larger N_t. The peak at the A^i_{1g} frequency mode is not affected by the beam size. The TLM band (not reported here) is slightly affected by the increase in the number of tubes.

IV. DISCUSSION AND CONCLUSION

To analyze the experimental data in the light of the calculated features of our work, in table I, we present, for some given experimental frequency (from references 7, 11 and 17) supposed as ω_{in}, the corresponding D_{in}, D_{out} and ω_{out}. The ω^S_{in} and ω^S_{out} represent the frequencies of RBLM modes for SWCNT inner and outer tubes respectively.

Bacsa *et al* [7] have reported the Raman spectrum of a DWCNT's sample that was assigned to single DWCNT with two peaks at 167 and 302 cm^{-1}. From our calculation, one can deduce that these peaks can be associated to DWCNT with inner and outer diameters around 7.95 and 14.79 Å. The calculated ω_{in} and ω_{out} are close to 299 and 166 cm^{-1} for interlayer distance 3.4 Å in good agreement with measurements.

The same analysis has been applied to the experimental results obtained by Bandow [17] on samples prepared by breaking the C_{60} molecules encapsulated in SWCNT's. From table I, for 488nm excitation, one can identify two DWCNT's (304:7.72, 166:14.51) and (384:6.12, 183:12.94) (cm^{-1}:Å) in agreement with experiment.

Recent Raman measurements on DWCNT's samples, obtained by direct synthesis method, performed by Cambedouzou [14], showed that the RBLM Raman spectrum is dominated by six peaks around 150, 166, 175, 265, 313 and 330 cm^{-1}. From our calculations, we assign these peaks to three single DWCNT's: 9.04 Å -15.84 Å, 7.47 Å-14.29 Å, and 7.18 Å -13.93 Å. From these values, a possible attribution of the DWCNTs can be proposed, corresponding to (9,4)@(15,8), (6,5)@(12,9) and (8,2)@(14,6) DWCNTs respectively. However, other DWCNT's can be compatible with the same experimental data. For instance, the calculations of the RBLM frequencies of (9,0)@(16,3) and (7,3)@(17,1) DWCNT also predict peaks located around 173 cm^{-1} and 330 cm^{-1}, close to the experimental data.

	(n,m)@(n',m')	ω^{in}_{exp}	D_{in}	ω^{out}_{cal}	D_{out}	ω^{out}_{exp}	ω^S_{out}	ω^S_{in}
(a)	(9,2)@(15,6)	**302**	7.95	166	14.79	**167**	153	282
(b)	(8,3)@(14,7)	**304**	7.72	166	14.51	**162**	155	291
	(5,4)@(11,8)	**384**	6.12	183	12.94	**182**	173	368
(c)	(9,4)@(15,8)	**265**	9.04	154	15.84	**150**	142	248
	(6,5)@(12,9)	**313**	7.47	169	14.29	**166**	157	301
	(8,2)@(14,6)	**330**	7.18	174	13.93	**175**	161	313

TABLE I: Estimated inner and outer diameters (in Å) and their corresponding frequencies (in cm^{-1}) calculated from the linear relationship (ω^S =225.1/D). The measured frequencies are considered as ω_{in}. (a) ref. [11], (b) ref. [10], (c) ref. [14].

In conclusion, we have investigated Raman spectrum of finite and infinite single and bundle of DWCNT's. An analysis of several experimental results performed on DWCNT's samples, in the light of nonresonant Raman spectrum within bond polarizability theory, has
been done with a good accuracy. Thanks to the spectral moments method, we have investigated DWCNT's with length greater than 500 Å and bundles consisting of more than 100 DWCNT's. Finite size effects (length and number of tubes) are observed essentially in the RBLM regions with additional modes which can be considered in analysis of experimental data.

ACKNOWLEDGMENTS

The computations were performed at CINES (Montpelier – France) as SP2 IBM computer. M.C acknowledges financial support from the CNRST – Morocco.

REFERENCES

[1] T. Sugai, H. Omote, S. Bandow, N. Tanaka, and H. Shinohara, J. Chem. Phys. 112, 6000 (2000).
[2] E. Flahaut, A. Peigney, Ch. Laurent, A. Rousset, J. Mater. Chem. 10 (2000) 249-252
[3] H. Zhu, C. Xu, B. Wei, D. Wu, Carbon 40 (2002) 2021-2041
[4] S. Bandow, M. Takizawa, H. Hirahara, M. Yudasaka, and S. Iijima, Chem. Phys. Lett.337, 48 (2001).
[5] M. S. Dresselhaus and P. C. Eklund, Adv. Phys. 49, 705 (2000).
[6] A. Rahmani, J.L. Sauvajol, S. Rols and C. Benoit, Phys. Rev. B 66, 125404 (2002).
[7] R. Bacsa, A. Peigney, C. Laurent, P. Puech, and W. S. Bacsa, Phys. Rev. B 65, 161404(R) (2002).
[8] A. M. Rao, E. Richter, S. Bandow, B. Chase, P. C. Eklund, K. A. Williams, S. Fang, K.
R. Subbaswamy, M. Menon, A. Thess, R. E. Smalley, G. Dresselhaus, and M. S. Dresslhaus, Science 275, 187 (1997).
[9] J. Kurti, G. Kresse, and H. Kuzmany, Phys. Rev. B 58, R8869 (1998).
[10] D. Sanchez-Portal, E. Artacho, J. M. Soler, A. Rubio, and P. Ordejon, Phys. Rev. B 59, 12678 (1999).
[11] L. Ci, Z. Zhou, X. Yan, D. Liu, H. Yuan, L. Song, J. Wang, Y.Gao, J. Zhou, W. Zhou, G. Wang and S. Xie, J. Phys. Chem. B 107, 8760 (2003).
[12] S. Rols, A. Righi, L. Alvarez, E. Anglaret, R. Almairac, C. Journet, P. Bernier, J. L. Sauvajol, A. M. Benito, W. K. Maser, E. Mutildenoz, M. T. Martinez, G. F. de la Fuente, A**.** Girard and J. C Ameline, Eur. Phys. J. B 18, 201 (2000).
[13] C. Benoit, E. Royer and G. Poussigue, J. Phys.: Condens. Matter 4, 3125 (1992).
[14] J. Cambedouzou, J.-L. Sauvajol, A. Rahmani, E. Flahaut, A. Peigney and C. Laurent, Phys. Rev. B 69, 235422 (2004).
[15] V. N. Popov and L. Henrard, Phys. Rev. B 63, 233407 (2001).
[16] V. N. Popov and L. Henrard, Phys. Rev. B 65, 235415 (2002).
[17] S. Bandow, G. Chen, G. U. Sumanasekera, R. Gupta, M. Yudasaka, S. Iijima, and P. C. Eklund, Phys. Rev. B66, 075416 (2002).
[18] A. Rahmani, J.L. Sauvajol, J. Cambedouzou and C. Benoit, Phys. Rev. B 71.125402 (2005).